Recent IBC Flight Test Results from the CH-53G Helicopter

Uwe T.P. Arnold
Director R&D
ZF Luftfahrttechnik GmbH
uwe.arnold@zf.com

Abstract

Since December 2001, ZFL has conducted Individual Blade Control (IBC) flight tests with a CH-53G testbed of the German Federal Armed Forces Engineering Center for Aircraft. The experimental IBC system used has been designed, manufactured, installed, certified, and tested by ZFL. This paper shows a comprehensive overview of the results from the concluded open loop and the just started closed loop campaigns. Vibration reduction turned out to be highly successful, especially with respect to the small required IBC authority. Without being explicitly optimized with respect to amplitude or phase, IBC was able to reduce the vibrations by more than 90% in a single axis or by more than 60% in all spatial directions in certain cases.

The noise experiments were focused on the reduction of BVI in descent flight conditions. With 2/rev IBC of 0.67 deg amplitude, noise reductions of up to 3 dB have been recorded. Following the trends known from prior wind tunnel experiments, the increased amplitudes, which are used during the closed loop campaign, should allow for even higher reductions. The positive impact of IBC on rotor performance at high forward speed was also successfully demonstrated. The simultaneous effect of IBC on both the rotor power and the flight condition corresponds to net power savings of up to 6% at 130kts forward speed. This means the application of optimum IBC not only reduces the rotor torque but also tends to increase forward speed and let the rotorcraft climb. The lower frequencies primarily used to reduce noise and power required also have considerable effect on the control system loads. In the optimum case encountered during the open loop tests, 2/rev IBC of the right phase was able to reduce the vibratory pitch link loads by more than 30%. Fortunately, it turned out that at high speed, the IBC input for optimum rotor performance also decreases the pitch link loads.

The last part of the paper gives an overview of the system modifications which had to be implemented for the closed-loop flight tests. It will be shown what control system architecture is available and what algorithms have been tested so far.

Notation

AFCS		Automatic Flight Control System
AccHGx, -y, -z	g	acceleration at main gearbox in x-, y-, z-direction
AccLadx, -y, -z	g	acceleration at cargo compartment in x-, y-, z-direction
AccPilx, -y, -z	g	acceleration close to pilot seat in x-, y-, z-direction
A_n	deg	*n*/rev IBC amplitude
BVI		Blade Vortex Interaction
FMEA		Failure Mode Effect Analysis
$G(...) = (x^2+y^2+z^2)^{1/2}$		unweighted cost function
g	m/s^2	9.81, gravity constant
HHC		Higher Harmonic Control
IBC		Individual Blade Control
J	-	Cost function to be minimized
N		6, number of blades
$\underline{T}_1$, $\underline{T}_2$	g/deg g/deg^2	IBC to vibration response transfer matrix (linear and nonlinear)
(M)TOW		(Maximum) Take-off Weight
P	kW	Power
Q	Nm	Rotor Torque
VIAS	kts	Indicated Air Speed
$\underline{u}$	deg	vector of higher harmonic control inputs (cos, sin, compon.)
$\underline{W}_i$		Weighting matrix with respect to i
$\underline{z}$	g	vector of vibrations and control loads (cos, sin compon.)
$\Delta\vartheta_{IBC}=\Sigma A_n cos(n\psi-\varphi_n)$		nominal pitch angle due to IBC
γ	deg	Flight path angle
φ_n	deg	*n*/rev IBC control phase angle
ψ	deg	rotor azimuth angle
Ω	rad/s	Rotor Speed

1 Introduction

ZF Luftfahrttechnik GmbH (ZFL) has designed, manufactured, certified, and tested a whole family of Individual Blade Control (IBC) systems using hydraulic blade root actuators. The most remarkable applications have been a flight-worthy system used still today on Eurocopter's BO-105 S1 testbed, see Ref. [7], as well as two powerful experimental systems used for full-scale wind tunnel tests of BO-105 and UH-60 rotors at NASA Ames, see Refs. [4] and [11] respectively. These campaigns have yielded a sound data base demonstrating the positive effect of IBC on vibrations, noise, rotor power required, and loads.

Based on the success of these programs ZFL was awarded a contract from the German Federal Office of Defense, Technology, and Procurement (BWB) to design, manufacture, install, qualify and flight test an IBC system for the medium weight transport helicopter CH-53G. With respect to the rotor design parameters this program is perfectly suited to complement the earlier IBC activities. The six-bladed fully articulated rotor of the CH-53G features a comparably high LOCK number but a small hinge offset and therefore differs considerably from the rotors investigated previously.

The test campaign is carried out at the German Federal Armed Forces Technical and Airworthiness Center for Aircraft (WTD 61) in Manching, where the certification authority is located, too. This facility operates the testbed, Fig. 1, and provides the full spectrum of technical and personnel support for data gathering, downlink, and recording as well as operation of the telemetry ground station. After the program had reached the last certification step with the final flight clearance, the open loop campaign had started December 19, 2001 with the first IBC inputs applied in flight.

Figure 1: IBC CH-53G testbed operated by WTD 61

In the German Armed Forces the medium lift VTOL capacity is based on a fleet of approximately 100 CH-53G helicopters. These rotorcraft now are in service for approximately 30 years and are scheduled to fly (however in reduced number) for another 25 years. This provides the motivation to consider suitable upgrades that can help to improve the performance and to contain the growing operation and maintenance costs for these ageing aircraft. The primary fields addressed and positively altered by the IBC for this aircraft are:

- Component fatigue and failure induced by high vibratory stress
- Unscheduled maintenance cost due to high vibration level
- CRTs of dynamical components determined by high (control system) loads
- Enabling of high TOW and/or high speed operation currently prohibited with regard to component life time constrains

Other benefits that can be expected through the application of IBC include:

- Reduction of power required or improvement of equivalent lift-to-drag ratio at high forward speed
- Significant reduction in noise radiation
- Automated in-flight tracking

The experience gained from the previous and the current test campaigns bolsters ZFL's view that IBC is a practical and valuable solution. It has retrofit capability and promises a high benefit-to-cost ratio.

2 IBC System

2.1 Basic System Architecture

For this IBC demonstrator program, ZFL has designed and manufactured all major hardware components as well as the control hard- and software. Ref. [9] gives a detailed description of the system layout. Key components of the IBC system are the six servo-hydraulic actuators mounted between the rotating swashplate and the blade pitch horns, compare Fig. 2 and 3.

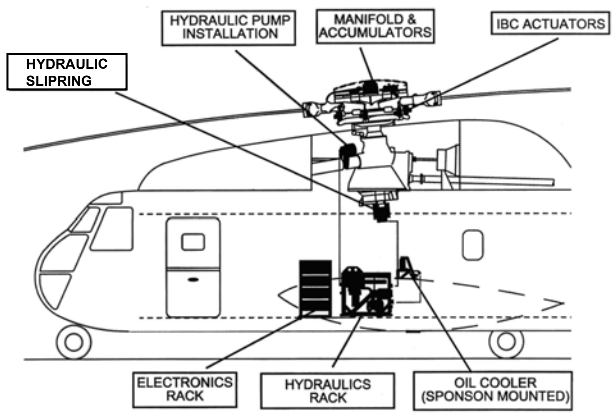

Figure 2: Integration of the IBC-System into the CH-53G Testbed

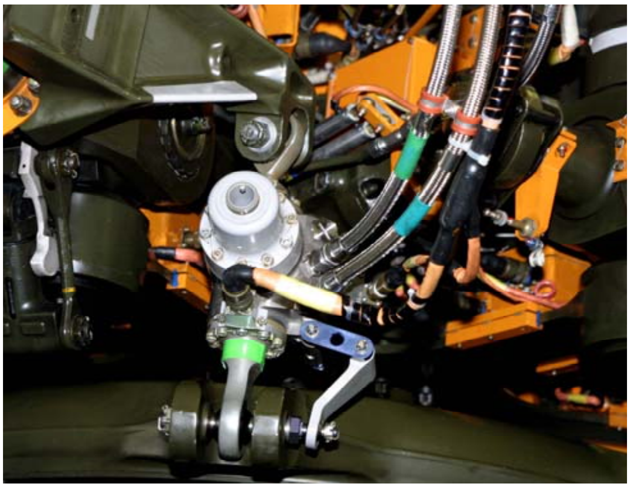

Figure 3: IBC Actuator Mounted between Swashplate and Blade Pitch Horn Replacing the Rigid Pitch Rod

Hydraulic power and electrical control signals are transferred via slip rings through the rotor shaft from the fixed frame to the hub. With regard to easy handling during the flight test operation and for minimal interference with the testbed, most of the hydraulic and control components are located in the cargo compartment of the fuselage. The hydraulic power supply for the IBC system is provided by two pumps mounted on the main gearbox input shafts. This follows from the requirement of complete separation of the experimental system from all basic aircraft systems.

2.2 Servo-hydraulic Actuator

Key component of the IBC System is the servo-valve controlled hydraulic blade root actuator. It replaces the conventional rigid pitch rod and imposes the desired relative motion between rotating swashplate and blade pitch horn with high bandwidth and accuracy. The basic specifications are given in Tab. 1.

max. piston stroke	+/- 6.7 mm
hard stops	+/- 1.27° blade pitch
usable amplitude	1.1° blade pitch
max. piston velocity @ design load	0.39 m/s
controlled frequencies	2/rev ... 7/rev
max. PLL dynamic/static	18.9 kN / 28.8 kN
lock-out force	> +/- 14 kN
break out force	> +/- 40 kN
lock-out time	< 100 ms
actuator mass	10.2 kg
system pressure	207 bar / 3,000 psi
hydraulic power available	49 kW
electrical power	0.6 kW

Table 1: System Specifications

Although the IBC System had to be sized to fit into the helicopter without major alterations, it needed to be powerful enough in terms of actuator amplitudes and forces to allow for full exploration of the IBC benefits.

2.3 Safety Concept

During the conceptual design special emphasis was put on the safety architecture. The IBC system has been designed to show fail-safe behavior. The FMEA has clearly proven the reliability required for certification. Although the components required to actively introduce IBC are partly of simplex design and driven by only one hydraulic power supply, the safety lock-out system is entirely duplex. This safety concept has also demanded a complete separation of the lock-out system. It is therefore mechanically as well as electrically separated from the rest of the IBC system. The sources used to trigger the lock-out procedure in case certain limits are violated include (a) IBC system parameters as position errors of the actuators, etc., (b) the aircraft reactions to IBC as blade flap and lead-lag angles, pitch link loads, gearbox and tail boom accelerations, etc. or (c) manual switches operated by the flight crew, see Fig. 4.

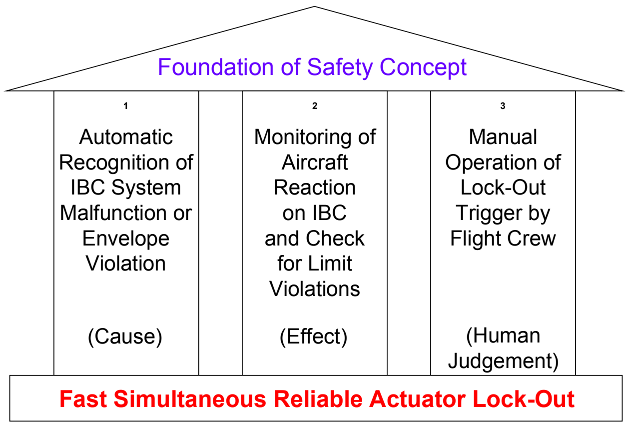

Figure 4: Three Column Safety Philosophy

When triggered, the control system is forced to fade out the periodic control functions and to command all actuators into their neutral position. More important, however, by opening a set of redundant valves in the hydraulic manifold a rapid depressurizing of the hydraulic system is assured. At all six actuators this leads to the release of the two independent safety locking pistons which mechanically catch the working piston and center it in its neutral position. The locking pistons are spring loaded and kept clear of the working piston by the hydraulic pressure itself. So any loss of system pressure - intentionally or accidentally - releases both locking pistons. The time from the trigger signal to the complete lock-out was repeatedly determined as one of the important parameters in each flight test stage. It typically stayed below 90 ms corresponding to approximately 90 deg rotor azimuth for all flight conditions.

2.4 Testbed

The CH-53G testbed 84+02 is operated by the WTD 61 since many years and had been used for a broad spectrum of test and certification issues for that helicopter type. Therefore, a comprehensive instrumentation did already exist with regard to flight mechanical parameters. Some 80 parameters are continuously measured with sampling rates of 119 or 476 Hz and recorded as PCM data stream on a DAT recorder.

With the installation of the IBC system some 100 additional parameters had to be processed. They stem from various sensors in the rotating frame which monitor the rotor operating condition (pitch, flap, lag angles, shaft and blade bending moments, control system loads, etc.) or the proper function of the IBC actuators (piston travel, pitch link and scissors loads). Additional sensors are placed in the fuselage which monitor the condition of the hydraulic system and the accelerations at different locations. Moreover, several internal states of the digital IBC controller boards in the rotor hub and in the fuselage are continuously recorded for safety reasons. All these signals are processed by the IBC measurement system, which is integral part of the IBC computer. The sampling rate is precisely synchronized to the rotor azimuth using 128 samples per revolution. Separate measurements are automatically or manually triggered and extend over a predefined period of time. All data are written to a flash disk for easy offline processing.

Both systems continuously exchange data via an analog interface. The IBC measurement system receives all parameters processed in the Data Gathering system while sending most of its own parameters to that system. This allows all safety relevant parameters of the IBC system to be included in one of the two data streams which are transmitted to the ground station for online monitoring.

2.5 Qualification and Certification

Before its integration into the testbed, the key IBC components as well as later the complete system underwent the usual series of development, qualification and certification tests. For this purpose ZFL had set up various test rigs, where the following issues have been experimentally investigated:

- Fatigue strength of IBC actuator and its scissors (five specimens, $>10^7$ load cycles each)
- Piston seal and bearing life under centrifugal loads (>1,250h)
- Functional reliability and endurance of actuator lock-out system (three actuators, >78,000 sequences over all)
- Lock-out time at low and high temperatures
- Reliability of shut-off manifold and hydraulic system

In a special component test rig a complete CH-53G flight control system had been set up. It consisted of an original swashplate, swashplate guide, IBC actuators and flap/lag hinges attached to a dummy rotor hub. Aerodynamic and inertial/centrifugal loads on the actuators were simulated by added springs and masses. The interaction of the IBC actuators with the primary control system and the change of control loads due to IBC operation was thoroughly examined. All components were equipped with strain gauges as still are the flying components for monitoring the in-flight loads.

After the qualification of the separate IBC components, the whole IBC system was tested on an iron bird. It consisted of a complete CH-53G quick change unit, i.e. main gear box, swashplate, rotor head assembly, and the associated hydraulic system. This system test has provided valuable insight into the dynamical behavior of the hydraulic system, especially the pressure pulsation during harmonic actuator operation and system lock-out. The testing of the fully equipped quick change unit also included the final acceptance test before it was installed in the testbed.

The whole certification process was guided by the Airworthiness Center for Military Aircraft at the WTD 61. The IBC system has been designed according to the applicable paragraphs of FAR Part 29, MIL T8679, MIL H8501 A, MIL Std 1629A, ADS-33D, and VG-95370. In addition, the following standards had to be followed for all components that constitute the lock-out system: MIL H5440 H, RTCA-DO160D, VG-95373. Flight clearance was granted step by step for progressive IBC authorities based on the experimental results of the preceding step.

3 Open Loop Flight Test Campaign

After the complete ground test certification procedure was accomplished, flight clearance for the first flight with IBC was granted in December 2001. In the first test phase hard stops were implemented that allowed for max. IBC amplitudes of 0.15 deg. The flights covered various system validation tests and the first investigation of the IBC benefits. Although primarily intended to serve as a certification milestone and to prove the basic IBC functionality it turned out that the effectiveness of IBC in affecting vibrations was so strong that valuable results could already be gathered with this small authority. Later during the test program the hard stops were stepwise changed to allow for amplitudes of 0.67 and finally 1.1 deg. Table 2 gives an overview of the various test conditions covered up to now.

All flight tests are conducted in close cooperation between WTD 61 and ZFL. WTD 61 provides all necessary support for the basic aircraft. This includes maintenance personnel, the complete flight crew, and the airport with its proven flight test infrastructure.

	Flight Condition	IBC Inputs (max. Amplitudes)					
		2/rev	3/rev	4/rev	5/rev	6/rev	7/rev
Certification Flights	HOGE	0.67°	0.67°	0.67°	0.67°	0.67°	0.67°
➢ EMC-Tests	40kts HF	0.67°	0.67°	0.67°	0.67°	0.67°	0.67°
➢ Lock-Out	60kts HF	0.67°	0.67°	0.67°	0.67°	0.67°	0.67°
➢ Interaction IBC/ AFCS	90kts HF	0.67°	0.67°	0.67°	0.25° *T*	0.25° *T*	0.25° *T*
	130kts HF	0.67°	0.67°	0.67°	0.25° *T*	0.25° *T*	0.25° *T*
Vibrations Pitch Link Loads	60kts HF	0.83°	0.67° *P, S*	0.15° *P*	0.15° *P, S*	0.15° *P*	
	90kts HF	1.10° *P*	0.67° *P, S*	0.40° *P, S*	0.25° *P, S*	0.25° *P, S*	0.25° *P, S*
	120kts HF	1.10° *P, S*	0.83° *P, S*	0.50° *P, S*	0.25° *P, S*	0.25° *P, S*	0.25° *P, S*
Noise	95kts HF	0.33° *P*					
	65kts DC -6°	0.67° *0°, 30°, 60°, 90°, 120°,240°*					
Power Required	130kts HF	0.67° *0°, 180°, 240°, 300°*					

P = Primary Phases: 0°, 60°, 120°, 180°, 240°, 300°, 359°
S = Secondary Phases: 30°, 90°, 150°, 210°, 270°, 330°
T = Test Phases: 0°, 90°, 180°, 270°

HF = Horizontal Level Flight
DC = Descend Flight

Table 2: Overview of IBC Flight Test Conditions

3.1 Open Loop Results

The results presented hereafter are derived from the data of the first two phases where actuator strokes corresponding to max. 0.15 and then 0.67 deg could be used. The standard procedure during the open loop tests was to pick one single frequency, keep the amplitude constant and vary the corresponding IBC input phase angle in 60 deg increments. Reference data points were taken before and after each phase sweep with the actuators both locked and unlocked but commanded to neutral position.

3.1.1 Actuator to Blade Transfer Function

The IBC system precisely controls the actuator stroke. Depending on the applied frequency the resultant blade pitch motion differs with regard to amplitude and phase from the geometrically expected value. Figure 5 compares the actuator stroke (expressed in terms of the corresponding nominal blade pitch angle) and the actually measured blade motion at that frequency.

It can be seen, that for 3/rev and 4/rev the blade motions tend to be higher than expected from a strictly geometric transfer of the actuator stroke, whereas at 5/rev and 7/rev the blade motions are considerably smaller. Moreover, phase deviations are present in all cases. The fact that at the higher frequencies the transfer function is quite independent from the IBC phase suggests that the impedance seen by the actuator is primarily of inertial nature. At the lower frequencies, however, the magnitude strongly depends on the IBC phase, showing a strong impact of the aerodynamics. In the most extreme case, a 2/rev actuator motion imposed with 300 deg IBC phase just cancels the 2/rev blade pitch motion component obviously present at this flight condition without IBC, whereas for 120 deg IBC phase that inherent 2/rev blade motion is more than doubled.

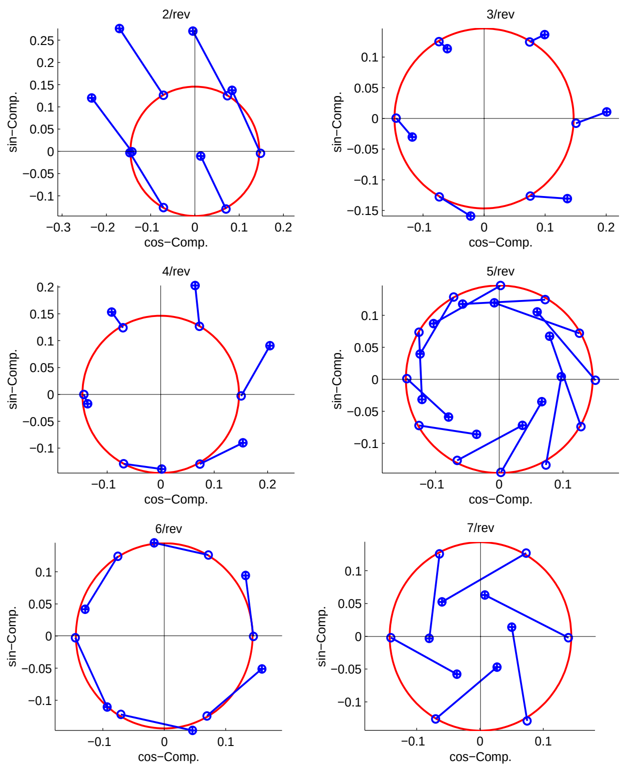

Figure 5: Blade Pitch Angle Response to IBC with Constant Actuator Stroke (2/rev ... 6/rev @ 120 kts and 7/rev @ 90 kts)

3.1.2 Vibration Reduction

The diagrams presented hereafter show the relevant 6/rev component of the measured parameter (as computed from FFT over 16 rotor revolutions) either by SIN/COS polar plots, by magnitude versus IBC phase angle plots or by frequency spectra. All data points were taken in straight level flight at approximately 4000 ft density altitude; the aircraft weight ranged from 75% to 85% of the CH-53G's 42,000 lbs MTOW. This compilation is solely intended to highlight some of the interesting effects and by no means comprehensive.

Before the first data had been evaluated it was assumed that the initial authority corresponding to +/-0.15 deg nominal blade pitch variation would hardly yield any usable data, since the impact on the vibrations was expected to be small. The data then processed, however, showed a very high effectiveness of IBC with respect to the vibrations, which was not modeled by any of the rotor codes used for prediction. Moreover, the recorded data are of high consistency even though the number of repeated data points was restricted. To make the data applicable to amplitude extrapolation and multiple frequency (i.e. mixed mode) predictions they were used to identify a second order T-matrix model (T^2-fit) according to the following relationship.

$$\underline{z} = \underline{\underline{T}}_1 \underline{u} + diag(\underline{u}) \underline{\underline{T}}_2 \underline{u} + \underline{z}_0$$

More details are given in Ref. [10]. This model has proven its ability to capture also most of the inherent nonlinear effects when using non-HHC frequencies (2/rev, 3/rev and 4/rev in the case of the six-bladed CH-53G). It is also used within one of the closed loop control algorithms

In the following diagrams Figs. 6 through 8 the 6/rev accelerations at two different sensor locations recorded during 0.15 deg 5/rev IBC phase sweeps are compared to the corresponding reference data without IBC.

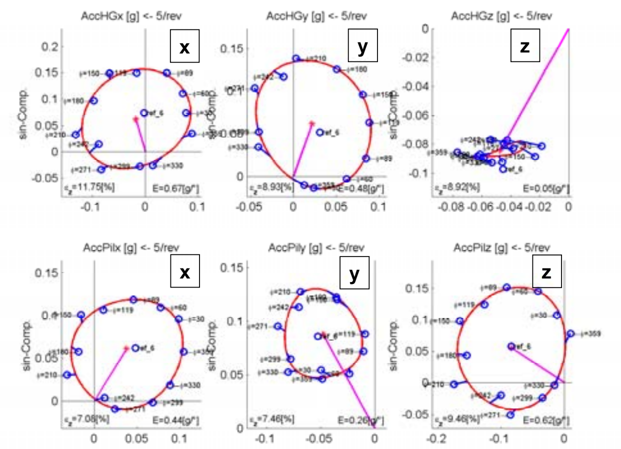

Figure 6: Measured 6/rev Accelerations at Main Gearbox and Pilot Seat due to 0.15 deg 5/rev IBC (120kts)

The added solid curves in Fig. 6 and 7 represent the identified T^2-fit. The values predicted by the identified model and the actual data points are connected by short lines representing the identification errors. It can be seen that all data can consistently be represented by the T^2-fit and the identification errors stay very small in most cases. Moreover, although not evaluated by the identification algorithm even the IBC-off values of the model match the measured reference data quite well. In this 5/rev case one finds four examples where the applied small IBC amplitudes were already sufficient to cancel a particular acceleration component. It must be noted, however, that for the simultaneous reduction of multiple vibration components at different locations the required 5/rev contribution to an optimized mixed mode signal can be somewhat higher.

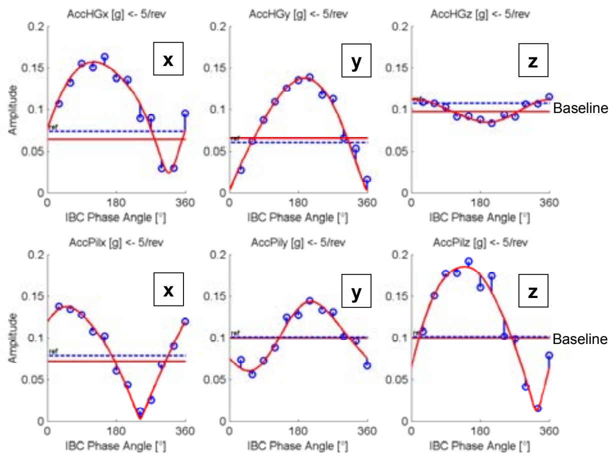

Figure 7: Measured 6/rev Accelerations at Main Gear-box and Pilot Seat due to 0.15deg 5/rev IBC vs. Phase Angle (120kts)

It should also be noted that in most cases from plots like Fig. 7 no final conclusions can be drawn with respect to the achievable vibration reduction and the optimum IBC phase angle unless the used amplitude happens to be the optimal one. Since the amplitudes have never explicitly been optimized during the open loop campaign, such impressive results like the almost complete cancellation of the vertical 6/rev component at the pilot seat as shown in Fig. 8 were recorded more by chance rather than by intention.

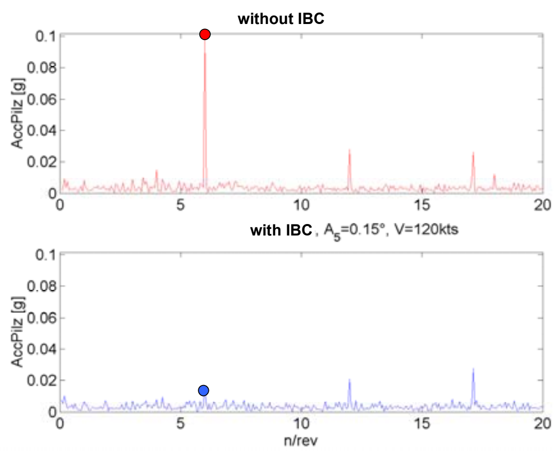

Figure 8: Effect of 0.15 deg 5/rev IBC on z-Vibration Spectrum at Pilot Seat (120kts)

Figures 9 and 10 show the influence of the two adjacent frequencies, 4/rev and 6/rev. It is worthwhile mentioning that 4/rev and 6/rev show similar effectiveness (for the definition of the effectiveness see Ref. [10]), although 4/rev is not a classical HHC frequency for the six-bladed rotor and would be ranked ineffective by linear first order analysis.

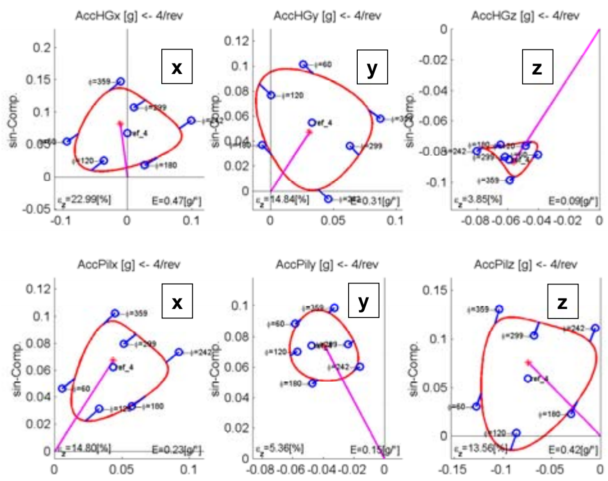

Figure 9: Measured 6/rev Accelerations at Main Gearbox and Pilot Seat due to 0.15 deg 4/rev IBC (120kts)

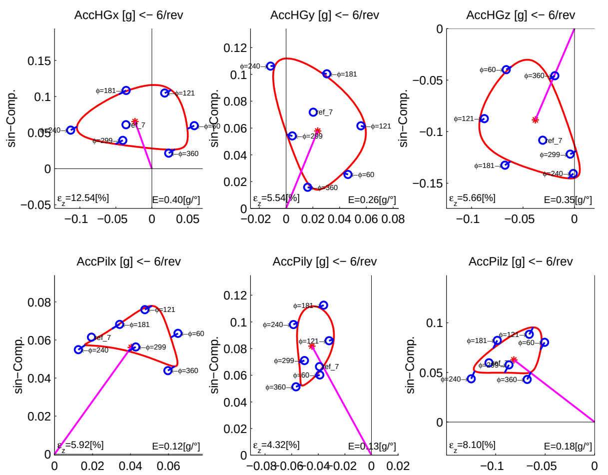

Figure 10: Measured 6/rev Accelerations at Main Gear-box and Pilot Seat due to 0.15 deg 6/rev IBC (120kts)

Figures 11 and 12 give an overview of the measured IBC effectiveness for all applied frequencies. Especially at the main gearbox the typical behavior can be observed that 5/rev and 7/rev IBC primarily affects the in-plane accelerations while 6/rev is more effective in the vertical axis. The fact that the non-HHC frequency 4/rev has considerable impact on the vibrations is again underlined. This frequency will later be shown to serve as valuable supplement in mixed mode cases. In general, the calculated IBC effectiveness with respect to the vibration reduction task reaches values of more than 0.6 g/deg, which is considerably higher than all values measured for the BO-105 or UH-60 helicopters.

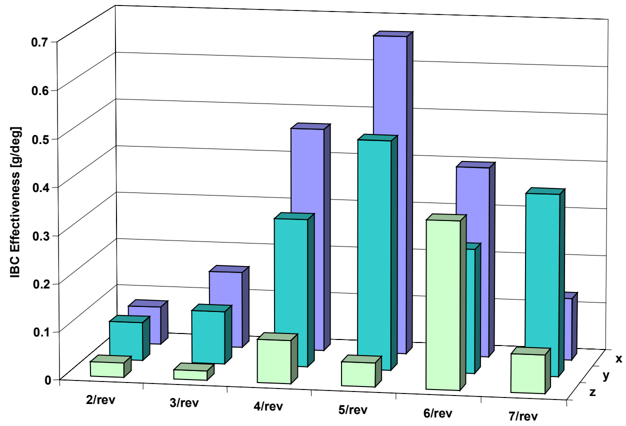

Figure 11: Effectiveness of Different IBC Harmonics at Main Gearbox (6/rev Acceleration per deg n/rev IBC; 120kts, 7/rev: 90kts)

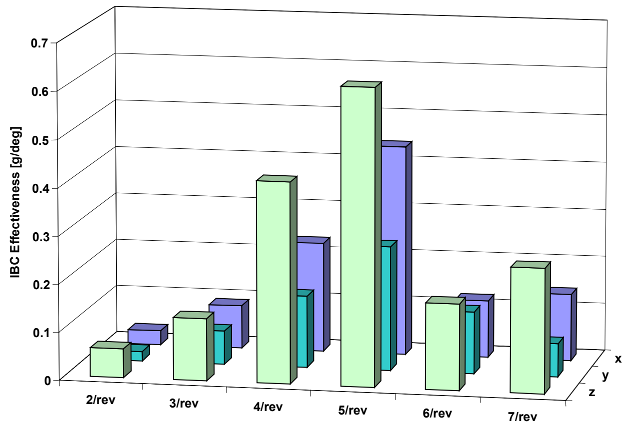

Figure 12: Effectiveness of Different IBC Harmonics at Pilot Seat (6/rev Acceleration per deg n/rev IBC; 120kts, 7/rev: 90kts)

As can be seen from the previous pictures, in many cases the optimum IBC amplitudes and phase angles for the three orthogonal sensor orientations or different sensor locations do not coincide. This becomes obvious as soon as the x, y, and z signals are combined into unweighted cost functions representing the spatial accelerations at the different locations, see Fig. 13.

Even though the deviating requirements for the different sensor directions and locations diminish the over-all results, the presented example shows that in some cases single harmonic IBC was able to lower the spatial vibrations at one location by more than 60% (cargo compartment) while the vibrations at the other observed locations were also reduced, however to a smaller extent. In other cases single harmonic IBC had divergent effects on different locations.

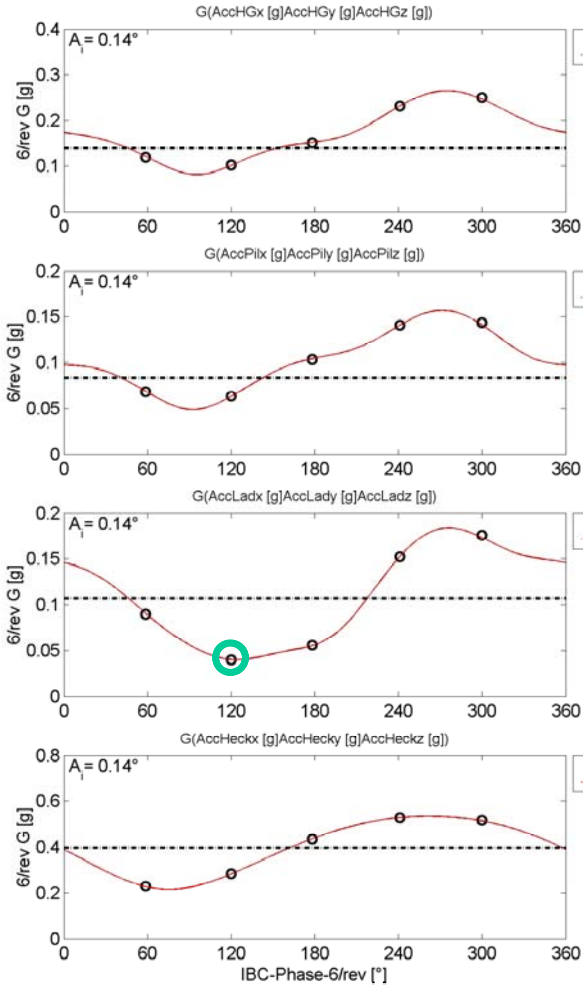

Figure 13: Effect Spatial 6/rev Accelerations at Four Sensor Locations Due to 0.15 deg 6/rev IBC (60kts)

3.1.3 Predicted Multiharmonic Effect

As shown in the previous section single harmonic IBC becomes less effective if one needs to reduce vibrations at different locations and multiple axes simultaneously. Therefore, the identified nonlinear T-matrix models were used to calculate optimum mixed mode inputs considering frequencies from 4/rev to 7/rev. In the following example the cost function consisted of the three equally weighted acceleration components x, y, z at the main gearbox or the pilot seat, respectively. Figure 14 shows the relative effect of different frequency combinations on the cost function as yielded by the numerical optimization.

The calculations confirm earlier findings partly already known from previous HHC and IBC programs.

- The important role IBC with (N-2)/rev can play is underlined (4/rev in this case)
- Applying more than one control frequency helps to tackle different sensor axes and/or locations simultaneously
- For the CH-53G the over-all authority required for the vibration reduction task seems to stay below 1 deg even for the suitable multi-harmonic inputs

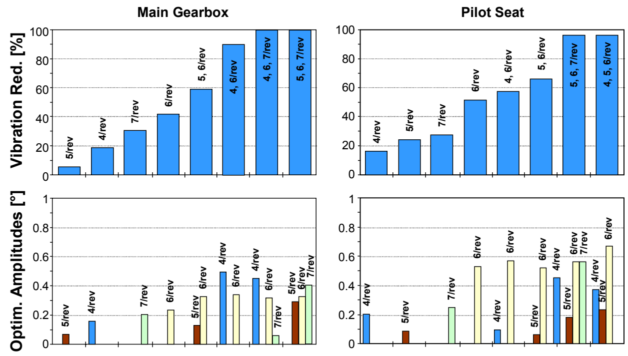

Figure 14: Predicted Spatial Vibration Reduction for Main Gearbox and Pilot Seat (120kts)

It can be seen that for this nonlinear extrapolation a mixture of three frequencies is sufficient to almost completely cancel the considered vibration components. These theoretical results will shortly be validated when optimized mixed mode IBC will be applied during the closed loop campaign.

3.1.4 Noise Reduction

As it has been shown in various investigations (e.g. Refs. [6], [7], [14]), noise radiation caused by the blade vortex interaction (BVI) phenomenon can be lowered by using 2/rev and/or 3/rev IBC. Thus, the effect of 2/rev IBC on the noise measured on ground was studied during the open loop campaign. As it has been shown in the previous section, 2/rev control was found to have only small impact on vibrations for this six-bladed rotor. Hence, 2/rev control was expected to be applicable without any severe drawbacks to the vibration reduction task.

The noise measurements were performed in close co-operation with the WTD 61 in a setup according to the ICAO regulations. Three microphones were placed in a line perpendicular to the flight path. Marks on the ground and a mobile GPS receiver supported the pilot in flying as exact as possible over the center microphone in the desired altitude. The flight path was tracked and recorded at a ground station by optical means. These data were used to give the crew instantaneous feedback on the quality of the flight path and later to correct the measured sound pressure levels according to the residual deviations. In addition to the ground measurements two external microphones had been mounted to the right sponson of the aircraft. It was intended to use their signals as an on-board indicator for the noise radiation of the rotor.

The following diagrams refer to the descent flight experiments only, for additional results from the horizontal fly-overs see Ref. [19]. Figure 15 shows the geometry of the descent flight path. A variation of ±10 m in altitude and ±25 m lateral deviation was tolerable (due to GPS and the ground marks, however, lateral deviations were much smaller). Otherwise, the flight was repeated. The altitude of the helicopter above the microphone line was used to correct the sound pressure level in order to get consistent data. A measurement distance of 500 m ahead and behind the microphone line had to be passed with the flight condition kept as steady as possible. The aircraft was expected to cross the microphone line in an altitude of 120 m. The IBC signal was faded in before the helicopter entered the measurement zone and was kept constant throughout the measurement. Based on preceding reference flights at different descent rates a flight path angle of -6° was found to produce the strongest BVI effect and therefore chosen for the IBC trials. This was in good agreement with the results from the IBC flight testing of the BO-105.

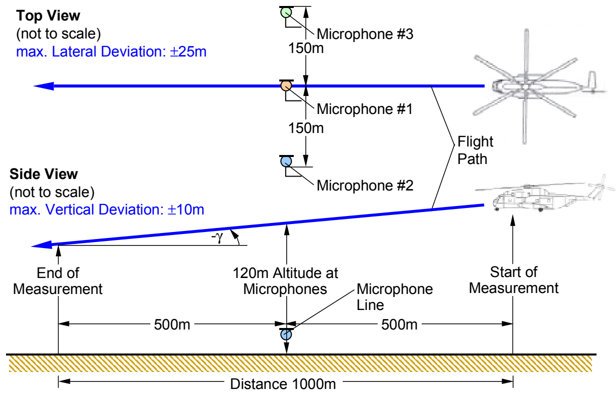

Figure 15: Descent Flight Path Geometry for Noise Reduction Flight Tests

Figure 16 shows the impact of 0.67 deg 2/rev IBC on the averaged sound pressure levels at the three microphones (center, retreating, advancing side) at 65 kts for various IBC phase angles. Without IBC the center microphones had recorded the highest levels. The maximum reduction was achieved at 30 deg IBC phase angle, when the sound pressure level at the center microphone was reduced by about 3 dB. This is an impressive result, given the relatively small amplitude of only 0.67 deg. Simultaneously, the sound pressure levels at the other two microphones were also reduced. This is important, since it clearly indicates an alleviation of the BVI effect, whereas for 60 deg phase angle, the sound pressure level was reduced at the center microphone, but increased on the retreating side pointing towards a change in directivity rather than an over-all reduction.

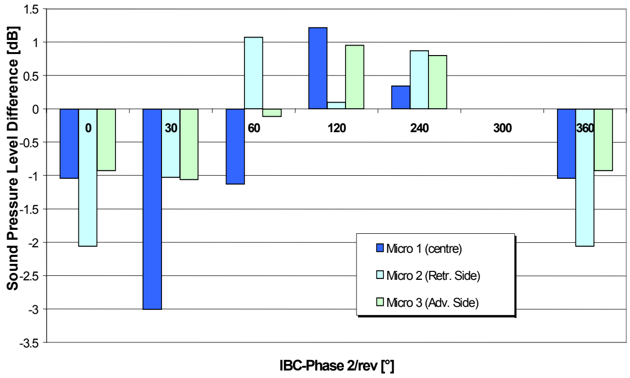

Figure 16: Effect of 0.67 deg 2/rev IBC on Measured Noise in Descent Flight Condition (65kts, 6deg Glide Slope)

From several studies it is known that higher levels of noise reduction can be expected, if higher amplitudes are applied. The analysis of IBC wind tunnel tests with respect to noise reduction given in [14] clearly shows falling sound pressure levels for increased IBC amplitudes. This implies that lower sound pressure levels can be expected also for the CH-53G when the noise measurements are repeated with the maximum authority of 1.1 deg.

Finally, Fig. 17 shows the comparison of sound pressure level time histories without and with IBC (A_2 = 0.67 deg, φ_2 = 30 deg). As can be seen, the sound pressure level is not only being reduced at all microphones, but also throughout almost the complete time history. This again points at an over-all reduction of the BVI strength.

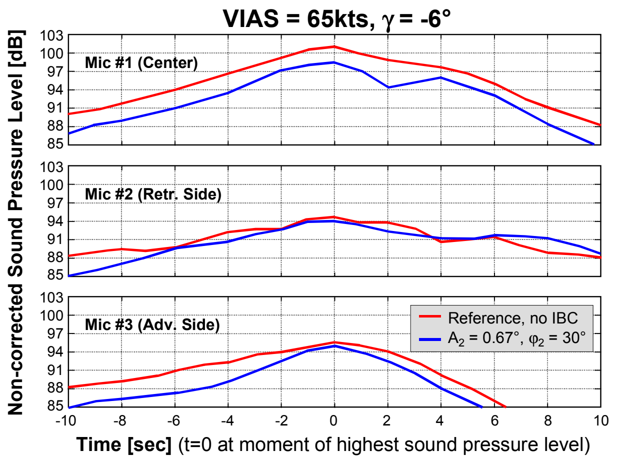

Figure 17: Effect of 2/rev IBC on Non-corrected Sound Pressure Level in Descent

3.1.5 Reduction of Power Required

It has long been accepted that 2/rev IBC can beneficially affect the rotor power required, see Ref. [5]

beside others. Therefore, 2/rev flight tests at high forward speed have also been evaluated with respect to this IBC application. Moreover, special flights have been devoted to this particular question. The general problem of resolving small power changes from flight test measurements also applies to the IBC experiments. Two approaches were used to assess the IBC effect on the main rotor power consumption. First, IBC phase sweeps were conducted in close sequence so that small changes of the flight condition introduced by the IBC inputs themselves had to be tolerated. Second, on-off sequences were performed, while the pilot was asked to retrim the aircraft as precisely as possible.

Figure 18 shows data taken according to the first approach. It can be seen that beside the measured shaft power also speed and altitude changed from data point to data point. This can be caused either by the varying IBC effect on torque, lift, and/or propulsive force or by the pilot's reaction on trim changes. The shown measurements were taken approximately 5 sec apart from each other and show very consistent trends. A second phase sweep with IBC phase angles shifted by 30 deg (φ_2 = 30, 90, 150, 210, 270, 330 deg) was used to supplement the shown first sequence.

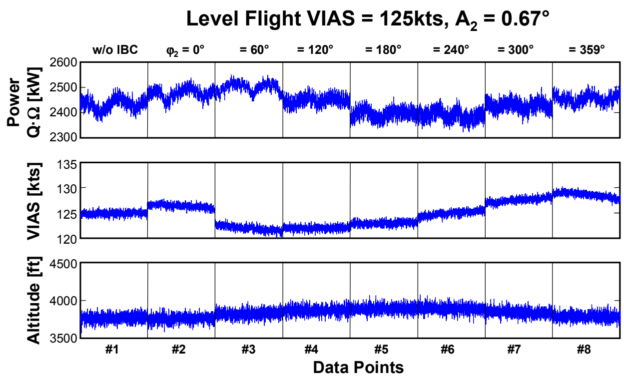

Figure 18: Flight Performance Relevant Parameters during 2/rev IBC Phase Sweep

Both runs consistently showed a power variation in the order of ±2 deg with the minimum at phase angles of approximately 240 deg, compare upper diagram of Fig. 19. Then, to consider the variation of the flight condition, correction factors have been computed, which translate the relevant deviations into equivalent power changes. The parameters used for these corrections comprise (a) the forward speed affecting the parasitic power, (b) the flight path angle representing the exchange of potential energy, and (c) the speed change representing the variation in kinetic energy. Simple energy relationships turned out to yield very similar results compared to more sophisticated analysis with a comprehensive helicopter performance code.

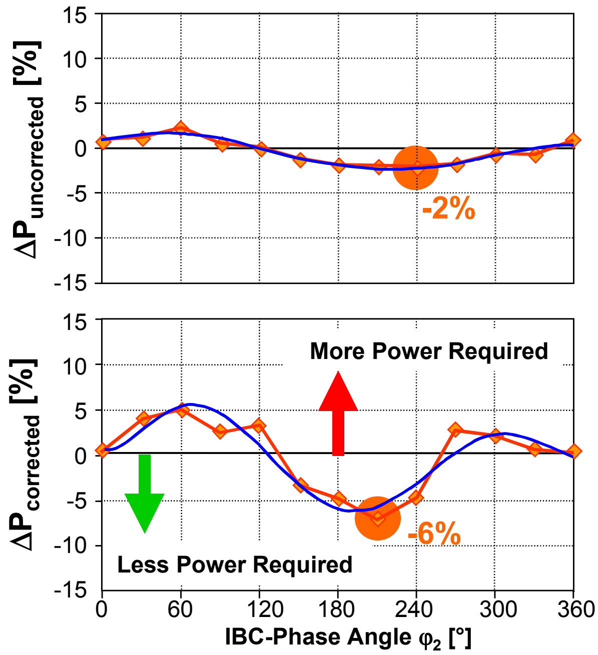

Figure 19: Rotor Power Reduction due to 0.67 deg 2/rev IBC (125 kts)

Figure 20 shows the corresponding power corrections that had to be applied to the shaft power measurements. The resulting power variation versus IBC phase angle is shown in the lower diagram of Fig. 19. At the optimum phase angle of now 210 deg a power reduction of more than 6% was found.

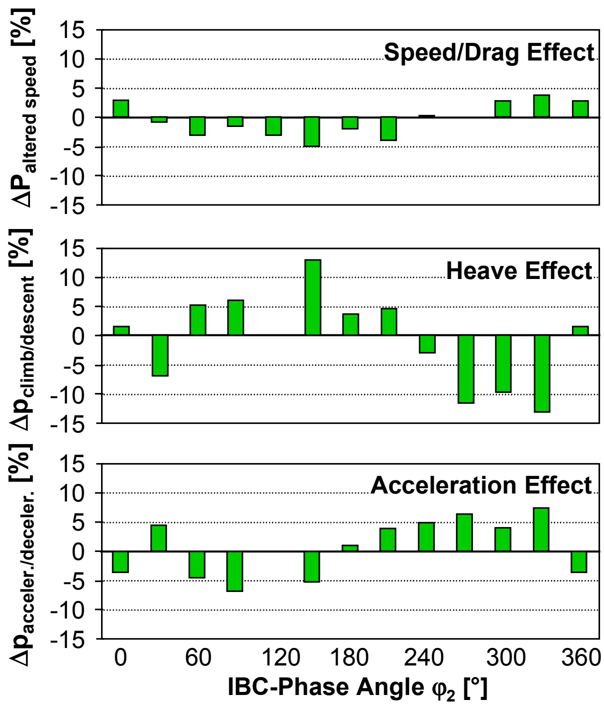

Figure 20: Power Corrections due to Flight Condition Changes

It is worthwhile mentioning that although the correction factors in some cases did develop differently during both phase sweeps (see phase angles 0, 30, 60 deg, e.g.) the trend of the corrected power is very consistent.

The second approach, used as benchmark only at the presumably optimum IBC phase angles, has yielded very similar power reductions with 3.1% at 180 deg and 4.2% at 240 deg.

3.1.6 Load Reduction

The last IBC benefit that has been investigated based on the conducted flight tests concerns the reduction of different loads. One known effect is the change of pitch link or rather actuator loads due to IBC, compare Ref. [5]. But many more components of the dynamic system are affected by the IBC inputs. For the ageing fleet of CH-53Gs this application will be of increased importance since approaching retirement times for rare and/or high priced components start to become a major concern.

It is well known that at higher forward speeds the pitch link loads are composed of significant portions of higher harmonic components, which considerably contribute to the peak-to-peak values relevant for the component life time. Therefore, the impact of the lower IBC frequencies on the corresponding components of the pitch link loads were studied. Again, the primary attention was put on single harmonic 2/rev results since the aerodynamic effects, which could beneficially be altered by IBC, were known to be most dominating at this frequency. Figure 21 shows the recorded pitch link load amplitudes versus the IBC phase angle.

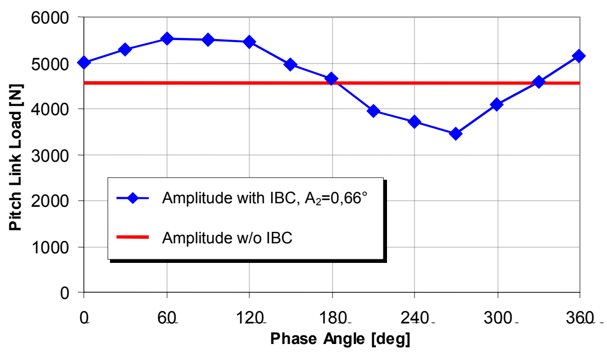

Figure 21: Effect of 0.66 deg 2/rev IBC on Pitch Link/Actuator Load Amplitudes (125kts)

At 270 deg phase angle the pitch link load amplitude was reduced by more than 25%. It should also be noted that at 210 deg, where the rotor power required was optimally reduced, the control system loads were still more than 15% below the reference value. The following time history plots underline the impressive IBC effect. Figure 22 shows the rise of the actuator axial forces after the beneficial 2/rev IBC signal was intentionally faded out. Figure 23 directly compares the control load time histories for two comparable data points without and with optimal IBC. In this case the load amplitude is reduced by more than 30%.

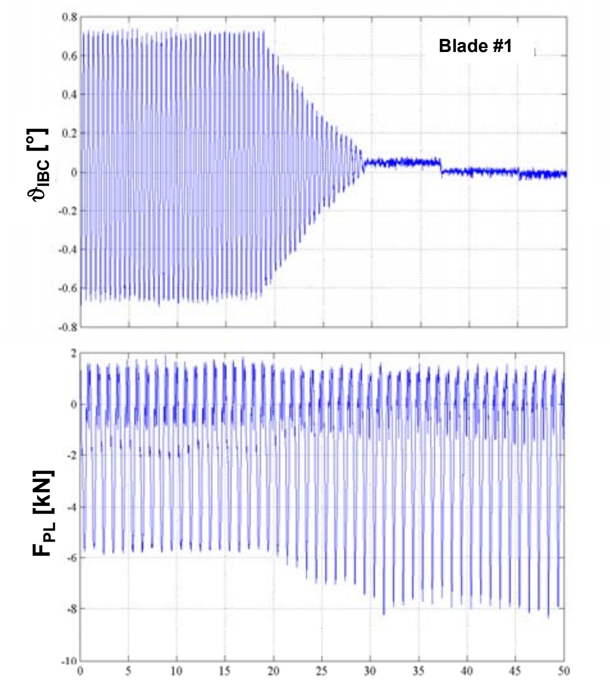

Figure 22: Effect of 0.66 deg 2/rev IBC on Pitch Link/Actuator Load Time History (Optimum Phase, IBC Fade-Out, 130kts)

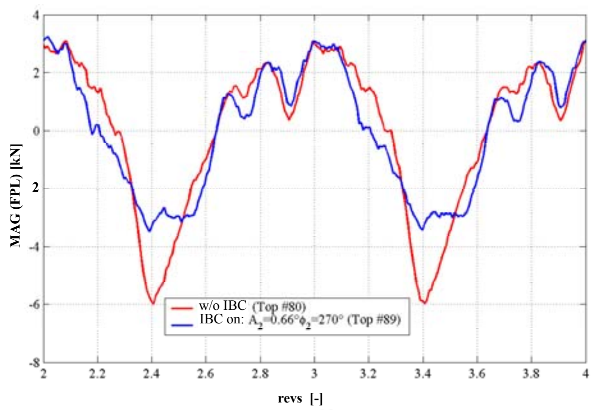

Figure 23: Effect of 0.66 deg 2/rev IBC on Pitch Link/Actuator Load Time History (over 2 Rotor Revolutions, Optimum Phase, 130kts)

As mentioned earlier, also other components in the rotor and control system load paths can be affected by IBC. Higher IBC frequencies tend to increase the loads due to the dominance of inertial effects. Fortunately, the application of such frequencies needed never to be restricted with regard to the load issue because of the small amplitudes required for the vibration reduction task. The lower frequencies, in contrast, could deliberately be used to reduce loads acting on certain critical components. Figure 24 shows the relative variation of three more sensor signals due to 2/rev and 3/rev IBC. Since the optimum phase angles do not coincide for all components, the cost function to be used by a feasible controller will have to combine different load measurements in an appropriate manner.

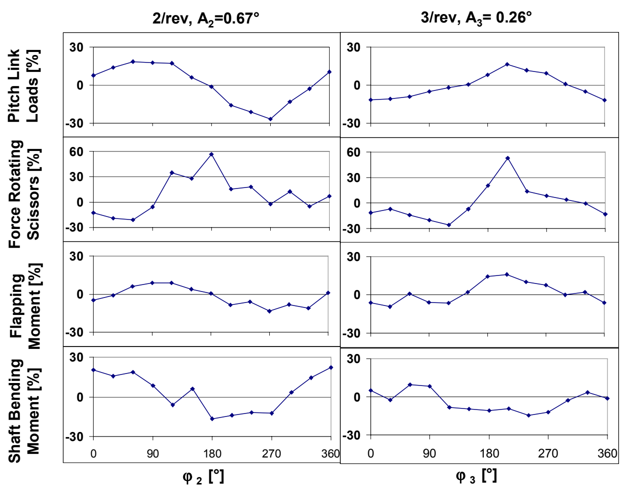

Figure 24: Relative Effect of 0.67 deg 2/rev and 0.26 deg 3/rev IBC on Different Rotating System Load Parameters

4 Closed Loop Flight Test Campaign

As expected from the beginning, the optimum IBC inputs considerably depend upon the flight condition. The predominant parameter was found to be the forward speed. Therefore, it will not be sufficient to use predefined sets of IBC inputs in a production version of an IBC system. Some years ago ZFL had started to investigate different candidates of control algorithms to be used for closed loop control, see Ref. [8]. Due to the success of the initial open loop tests ZFL was awarded an extension of the original contract which covers the development and flight testing of such a closed loop IBC system.

4.1 Control System Architecture

To retain the open loop core system with all its safety features a separate control computer was added to the existing open loop system which forms an additional outer control loop and allows to test different frequency domain algorithms. Thus, the closed loop hardware added to the existing IBC system extends the existing cascade control structure of the present IBC system by an additional control loop, as shown in Fig. 25.

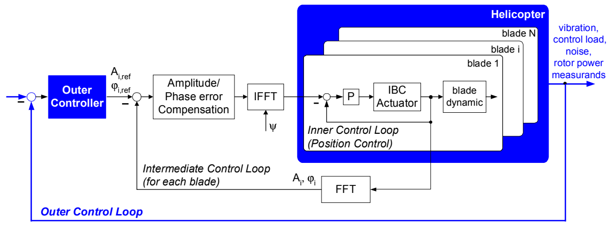

Figure 25: Control System Structure of Closed Loop IBC System

The open loop core system was altered only where necessary to communicate with the closed loop control computer. This approach was essential in minimizing the certification effort, since the inputs of the controller can now be treated very similar to the manual inputs of the former human IBC operator. The sensor signals required for feedback were already available in the data recording portion of the open loop IBC system.

The main interface between the closed loop hardware and the open loop system is the link which continuously transmits the commanded amplitude and phase values of the chosen IBC frequencies. What was done manually by the flight test engineer during the open loop flight tests is now provided by the closed loop control computer. To control the test procedure during the flight an additional man/machine interface has been designed. The closed loop control system consists of a modular dSPACE hardware system, a TFT-Touch screen and a Host-PC. The controller design is performed under Matlab/Simulink and automatically implemented on the dSPACE real-time system from block diagram level. The modified IBC system is capable of generating single and mixed mode IBC inputs that consist of arbitrary combinations of harmonics from 2/rev – 7/rev. The highest control update rate feasible with the extended IBC system is 4/rev.

The closed loop control algorithms used to form the outer control loop for the vibration and control load reduction tasks are based on the well-known frequency domain approach, compare Refs. [8] and [15] through [18]. The frequency domain approach assumes a quasi-static linear relationship between the outputs (measured vibrations and control loads) and the corresponding sets of IBC inputs. This relationship is formed by the so-called T-matrix model. The inputs are characterized by the cosine and sine parts of the 2/rev – 7/rev components of the IBC-input. The vibrations are composed of the $N\Omega$ components of accelerations measured at different locations (pilot seat, main gearbox, cargo compartment and tailboom). For the reduction of control loads suitable frequency components of measured pitch link and booster loads are used instead.

The over-all outer control loop used for the vibration and control load reduction consists of two main tasks. A system identification task used to estimate the T-matrix model and a controller task used to calculate IBC inputs to accomplish the desired control goal. The system identification can be performed using different Recursive Least Square methods (standard RLS, RLS with forgetting factor, different stabilized RLS methods) or Kalman filter implementations. The system identification task is able to estimate de-coupled T-matrix sub-models. If for example vibration and control loads shall simultaneously be addressed, the impact of 2/rev IBC on all vibration components can be neglected in the identification algorithm. Using this feature it is possible to neglect small cross-coupling effects in the controller design. Therefore selected IBC frequencies can be used to control specified outputs. Within the controller task the computation of IBC inputs is realized by minimizing

$$J = \underline{z}_n^T \underline{\underline{W}}_z \underline{z}_n + \underline{u}_n^T \underline{\underline{W}}_\vartheta \underline{u}_n + \Delta\underline{u}_n^T \underline{\underline{W}}_{\Delta\vartheta} \Delta\underline{u}_n$$

along with the identified T-matrix model

$$\underline{z}_n = \underline{z}_{n-1} + \underline{\underline{\hat{T}}}_1 \left(\underline{u}_n - \underline{u}_{n-1}\right)$$

where the subscript n denotes the current time step. The solution of the above optimization problem is either formulated using the feedback of measured values of $\underline{z}_n$ or using feedback of the identified reference values. The IBC-frequencies 4 through 7/rev are preferred for the vibration reduction and 2/rev IBC is reserved for the control system load reduction. Due to the different implementations of the system identification and the controller tasks the outer control loop can be realized with the following structures: non-adaptive closed loop, adaptive closed loop, non-adaptive feed forward; and adaptive feed forward.

4.2 Closed Loop Ground Test Results

In order to validate the function of the closed loop hard- and software, special tests have been performed not only with the system test rig but also with the testbed helicopter during ground test runs. Because no useful acceleration signals were available during these tests (rigid test rig or fuselage on the ground), a servo (booster) force of the primary control system was chosen as the parameter to be controlled by 6/rev IBC. Figures 26 and 27 show control sequences as recorded during these tests.

In the first case, Fig. 26, the plotted time histories comprise both the identification and the control time frames. For this test, an artificial 6/rev disturbance signal was superimposed to the measured servo force. It can clearly be seen, how this force component reacts on the automated phase sweep which is invoked as part of the identification process. Then, within less than 4 sec the controller has converged to the optimum 6/rev amplitude and phase values which perfectly cancels the fictitious servo load.

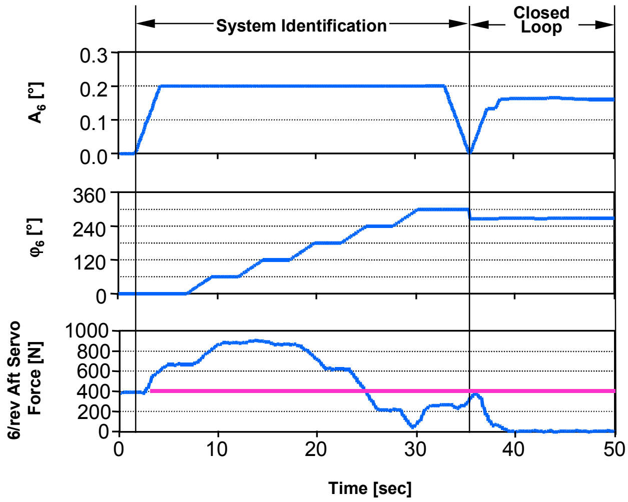

Figure 26: Closed Loop Test Carried out at Full Scale System Test Rig (Artificial 6/rev Aft Servo Force Suppressed by 6/rev IBC), from [19]

For the ground tests shown in Fig. 27, no dummy signals had to be added, since sufficient 6/rev signal content was present. In this case only the closed loop time frame is shown. Again, it can be seen, how fast and reliable the algorithm converges, before at the end of the sequence IBC is switched off and the cost function jumps up to the initial reference value. Based on these successful tests a stable and efficient controller performance is expected also for the upcoming flight tests.

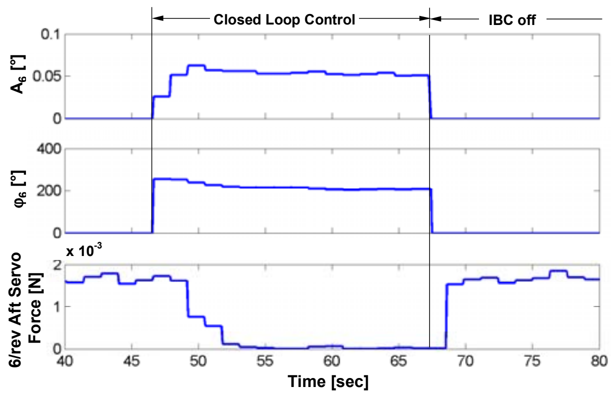

Figure 27: Closed Loop Test Carried out during a Ground Test Run (6/rev Aft Servo Force Suppressed by 6/rev IBC)

5 Conclusions and Outlook

This ongoing flight test campaign on the CH-53G has already demonstrated the potential of IBC to improve the rotor properties with respect to vibrations, noise, power required, and control loads. The results presented above are very encouraging and confirm the findings in [13]. The mixed mode extrapolations are still to be validated during the upcoming closed loop flight tests. The effectiveness of IBC with respect to the vibration reduction task has clearly surpassed prior expectations. The major results can be highlighted as follows:

- More than 60% vibration reduction at the cargo compartment through 5/rev single mode IBC has been demonstrated with simultaneous, however smaller, improvements at all other evaluated locations
- Local vibration reductions of more than 90% have been predicted by the non-linear T-matrix model for the application of mixed mode IBC
- The authority required for optimum mixed mode vibration reduction is not expected to exceed 1 deg
- In landing approach noise reductions of up to 3dB have been shown using 0.67 deg 2/rev IBC
- In high speed level flight the effective rotor power required was reduced by up to 6% again using 0.67 deg 2/rev IBC
- At the same speed pitch link load reductions of approximately 30% were measured for appropriate 2/rev IBC inputs
- Simultaneous power and control load reduction can be realized because the optimum 2/rev IBC phase angles were found to be sufficiently close

One primary advantage of the IBC concept is that different deficiencies of a helicopter rotor operating in tangential flow can be treated simultaneously by one single system. It is obvious, however, that an IBC retrofit kit will have to be optimized with respect to weight, cost and installation effort compared to the described experimental system. The latter was primarily designed to be an experimental tool for maximum flexibility and minimum interference with the testbed. The design goals for a production version are low weight, low power consumption, and small installation space as well as reliable function and autonomous operation. ZFL has pursued several design studies for different helicopters, not only by varying details of the mechanical integration but also under consideration of alternative methods for the power supply.

One preliminary design for the CH-53G shows a highly integrated solution weighing below 1% of the helicopter MTOW. It features the complete integration of all mechanical and hydraulic components in the rotating frame, see Fig. 28. This architecture removes the need for a hydraulic slipring. The pump is driven by the rotor itself and does not need an extra power pickup.

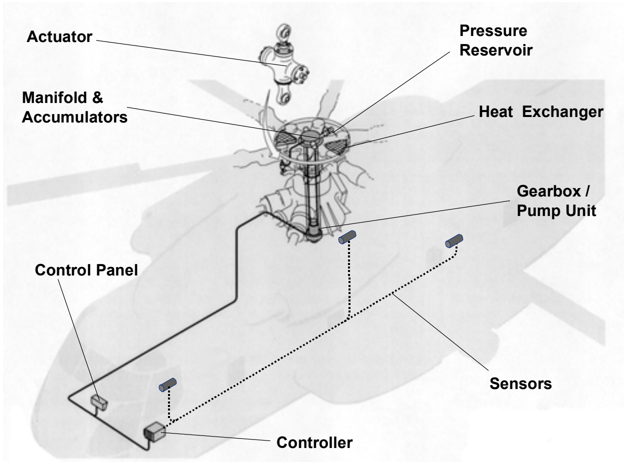

Figure 28: Possible Layout Variant of IBC Retrofit Kit

A further simplification of the IBC system could be realized if the design would consider the IBC-specific load / piston travel characteristics. Flight and wind tunnel test data have shown that the average mechanical power consumed by each actuator is comparably low, because the energy flow reverses during a considerable part of each rotor revolution. Thus, the power demand of IBC could be drastically reduced if a "regenerative" IBC system was designed that allows for power recovery.

There are several technical solutions which follow this idea. One solution, the so-called IBC displacement system, is currently being tested at ZFL. This system does not rely on the servo valve principle but directly connects a variable displacement pump with specialized actuators. This setup enables the desired bi-directional energy flow between the actuator and the pump. The regenerative IBC displacement demonstrator has meanwhile proven the validity of this concept and is now being optimized in detail. This technical approach can greatly simplify the IBC system layout and may help to introduce IBC into existing or new helicopters.

Acknowledgement

The work presented in this paper has primarily been funded by the German Federal Office of Defense, Technology, and Procurement (BWB). The author also likes to thank the staff of the German Federal Armed Forces Technical and Airworthiness Center for Aircraft in Manching (WTD 61) for their continuous support of this successful IBC campaign.

References

[1] P. Richter, H.-D. Eisbrecher, V. Klöppel, “Design and First Tests of Individual Blade Control Actuators”, 16th European Rotorcraft Forum, 1990.

[2] W. R. Splettstoesser et al., “BVI Impulsive Noise Reduction by Higher Harmonics Pitch Control: Results of a Scaled Model Rotor Experiment in the DNW”, 17th European Rotorcraft Forum, Berlin, 1991.

[3] D. Teves, V. Klöppel, P. Richter, “Development of Active Control Technology in the Rotating Frame, Flight Testing and Theoretical Investigations”, 18th European Rotorcraft Forum, Avignon, 1992.

[4] S. A. Jacklin, A. Blaas, S. M. Swanson, D. Teves, “Second Test of a Helicopter Individual Blade Control System in the NASA Ames 40-by-80 feet Wind Tunnel”, 2nd AHS International Aeromechanics Specialists Conference, 1995.

[5] U.T.P. Arnold, M. Müller, P. Richter, “Theoretical and Experimental Prediction of Individual Blade Control Benefits”, 23rd European Rotorcraft Forum, Dresden, 1997.

[6] S.M. Swanson, S.A. Jacklin, A. Blaas, G. Niesl, R. Kube, “Acoustic Results from a Full-Scale Wind Tunnel Test Evaluating Individual Blade Control”, 51st AHS Annual Forum, Fort Worth, 1995.

[7] D. Schimke, U.T.P. Arnold, R. Kube, “Individual Blade Root Control Demonstration - Evaluation of Recent Flight Tests”, 54th AHS Annual Forum, Washington D.C., 1998.

[8] D. Morbitzer, U.T.P. Arnold, M. Müller, “Vibration and Noise Reduction through Individual Blade Control Experimental and Theoretical Results”, 24th European Rotorcraft Forum, Marseille, 1998.

[9] O. Kunze, U.T.P. Arnold, S. Waaske, “Development and Design of an Individual Blade Control System for the Sikorsky CH-53G Helicopter”, 55th Annual Forum of the American Helicopter Society, Montreal, 1999

[10] M. Müller, U.T.P. Arnold, D. Morbitzer, “On the Importance and Effectiveness of 2/rev IBC for Noise, Vibration and Pitch Link Load Reduction”, 25th European Rotorcraft Forum, Rome, 1999

[11] A. Haber, S.A. Jacklin, G. deSimone, “Development, Manufacturing, and Component Testing of an Individual Blade Control System for a UH-60 Helicopter Rotor”, AHS Aerodynamics, Acoustics, and Test and Evaluation Technical Specialists Meeting, San Francisco, 2002

[12] P. Richter, W. König, “Einzelblattsteuerung (IBC) für den Transporthubschrauber CH-53G“, Deutscher Luft- und Raumfahrtkongress, Hamburg, 2001

[13] U.T.P. Arnold, G. Strecker, “Certification, Ground and Flight Testing of an Experimental IBC System for the CH-53G helicopter”, 58th Annual Forum of the American Helicopter Society, Montreal, 2002

[14] S.A. Jacklin, A. Haber, G. de Simone, et al., “Wind Tunnel Test of a UH-60 Individual Blade Control System for Adaptive Performance Improvement and Vibration Control“, 58th Annual Forum of the American Helicopter Society, Montreal, 2002

[15] W. Johnson, W., “Self-Tuning Regulators for Multicyclic Control of Helicopter Vibrations”, NASA Technical Paper No. 1996, 1982.

[16] G. Lehmann; R. Kube, “Automatic Vibration Reduction at a Four Bladed Hingeless Model Rotor – A Wind Tunnel Demonstration”, Vertica Vol. 14, No. 1, pp. 69-86, 1990.

[17] T. Millot, W. Welsh, “Helicopter Active Noise and Vibration Reduction”, 25th European Rotorcraft Forum, Rome, 1999.

[18] D. Fürst, T. Auspitzer, M. T. Höfinger, B. G. van der Wall, “Numerical Investigation of Vibration Reduction Through IBC for a 20to Helicopter Rotor Model”, 28th European Rotorcraft Forum, Bristol, 2002

[19] C. Kessler, D. Fürst, U. Arnold; “Open Loop Flight Test Results and Closed Loop Status of the IBC System on the CH-53G Helicopter”, 59th Annual Forum of the American Helicopter Society, Phoenix, Arizona, 2003